Earth and Planetary Science Letters 451 (2016) 97–107

Contents lists available at ScienceDirect

Earth and Planetary Science Letters

www.elsevier.com/locate/epsl

Complex deformation in western Tibet revealed by anisotropic tomography

Heng Zhang [a,b,*], Junmeng Zhao [a,c], Dapeng Zhao [d], Chunquan Yu [b], Hongbing Liu [a,c], Zhaoguo Hu [e]

[a] Laboratory of Continental Collision and Plateau Uplift, Institute of Tibetan Plateau Research, Chinese Academy of Sciences, Beijing 100085, China
[b] Department of Earth, Atmospheric and Planetary Sciences, MIT, Cambridge, MA 01239, USA
[c] CAS Center for Excellence in Tibetan Plateau Earth Sciences, Beijing 100101, China
[d] Department of Geophysics, Tohoku University, Sendai 980-8578, Japan
[e] Shandong Zhengyuan Institute of Geological Exploration, China Central Bureau of Metallurgy and Geology, Jinan 250000, China

ARTICLE INFO

Article history:
Received 18 November 2015
Received in revised form 5 July 2016
Accepted 11 July 2016
Available online 27 July 2016
Editor: A. Yin

Keywords:
anisotropic tomography
Tibetan plateau
lateral heterogeneities
diverse deformation patterns
crustal and uppermantle structures

ABSTRACT

The mechanism and pattern of deformation beneath western Tibet are still an issue of debate. In this work we present 3-D P- and S-wave velocity tomography as well as P-wave radial and azimuthal anisotropy along the ANTILOPE-I profile and surrounding areas in western Tibet, which are determined by using a large number of P and S arrival-time data of local earthquakes and teleseismic events. Our results show that low-velocity (low-V) zones exist widely in the middle crust, whereas low-V zones are only visible in the lower crust beneath northwestern Tibet, indicating the existence of significant heterogeneities and complex flow there. In the upper mantle, a distinct low-V gap exists between the Indian and Asian plates. Considering the P- and S-wave tomography and P-wave azimuthal and radial anisotropy results, we interpret the gap to be caused mainly by shear heating. Depth-independent azimuthal anisotropy and high-velocity zones exist beneath the northern part of the study region, suggesting a vertically coherent deformation beneath the Tarim Basin. In contrast, tomographic and anisotropic features change with depth beneath the central and southern parts of the study region, which reflects depth-dependent (or decoupled) deformations there. At the northern edge of the Indian lithospheric mantle (ILM), P-wave azimuthal anisotropy shows a nearly east-west fast-velocity direction, suggesting that the ILM was re-built by mantle materials flowing to the north.

1. Introduction

Although many controversial issues remain in the geodynamic models about the Tibetan plateau, the northward subduction of the Indian plate has been certainly playing a key role during the formation of the plateau. By using different techniques and data sets collected from several seismic experiments, such as the PASSCAL, INDEPTH, Hi-CLIMB, Namche Barwa, TW-80 and TIBET-31N, a number of seismic studies have been made to detect the subducting Indian plate beneath the Tibetan plateau and surrounding regions. Because of the complex structures of the Tibetan plateau and the sparse seismometer deployment, there are still many disputes on the northern limit and detailed deformation pattern of the Indian lithospheric mantle (ILM), e.g., whether the ILM is downwelling at the Bangong–Nujiang suture in central Tibet (Tilmann et al., 2003), whether the sub-horizontal ILM is underthrusting to the Jinsha River suture in western Tibet (Zhao et al., 2010), and whether the whole Tibet is underlain by relatively high-velocity materials (Priestley et al., 2006). Seismic anisotropy has been observed in various parts of the Earth's interior, including the crust, the upper mantle, the transition zone, the D" layer, and the inner core. Studies of seismic anisotropy can provide important constraints on both the past and present-day deformations beneath the Tibetan plateau. In general, the convergence of continents can cause strong deformations. Seismic anisotropy has been used to reveal the deformations and to identify the boundary between the ILM and the Eurasian lithospheric mantle (Huang et al., 2000).

The following geophysical features have been revealed in the Tibetan Plateau: (1) P and S wave velocities (Vp, Vs) are low in the north but high in the south (e.g., Zhang et al., 2012a, 2012b); (2) Sn-wave generation is inefficient in the north but efficient in the south (Rapine et al., 1997); (3) seismic anisotropy is strong in the north but weak in the south (Huang et al., 2000). These

* Corresponding author.
E-mail address: zhangheng415@itpcas.ac.cn (H. Zhang).

http://dx.doi.org/10.1016/j.epsl.2016.07.020
0012-821X/

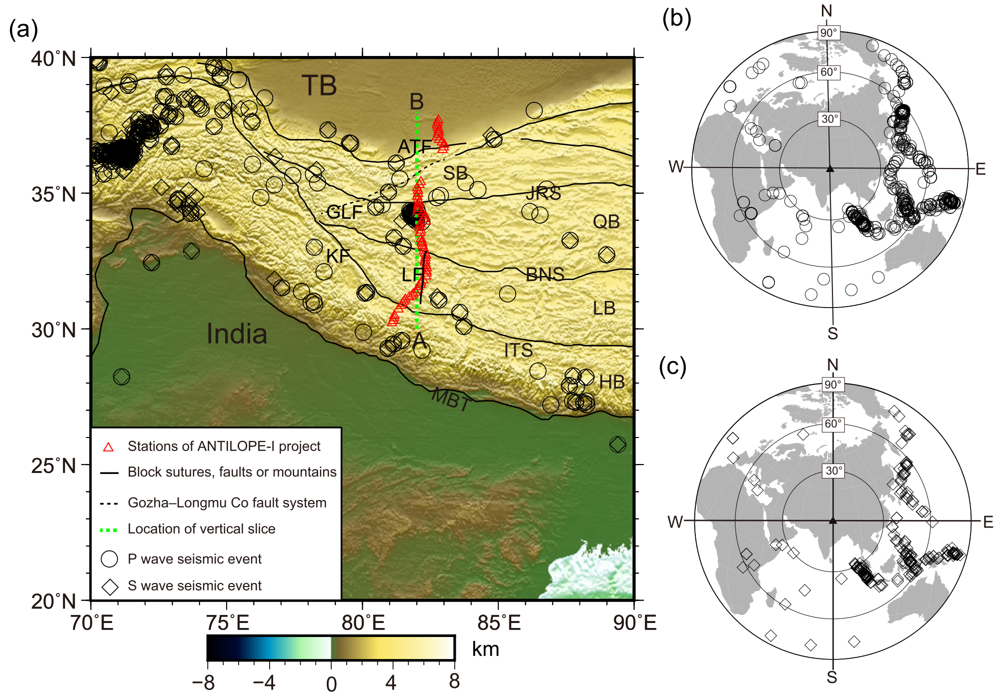

Fig. 1. (a) Map of the study region. The black lines denote the tectonic block boundaries. The red triangles show the portable seismic stations of the ANTILOPE-I project. The open circles and diamonds denote the local earthquakes generating P- and S-wave data, respectively. The green dashed line (A-B) shows the location of the vertical cross-section in Fig. 6. MBT, the Main Boundary Thrust; ITS, the Indus–Tsangpo suture; BNS, the Bangong–Nujiang suture; JRS, the Jinsha River suture; ATF, the Altyn–Tagh Fault; GLF, the Gozha–Longmu Co fault system; KF, the Karakorum fault; LF, the Lungar fault; HB, the Himalaya block; LB, the Lhasa block; QB, the Qiangtang block; SB, the Songpan–Ganzi block; TB, the Tarim basin. (b, c) Distribution of the teleseismic events at epicentral distances of 30°–90° which generated (b) P-wave and (c) S-wave data used in this study. (For interpretation of the references to color in this figure legend, the reader is referred to the web version of this article.)

features reflect strong lateral heterogeneities beneath the Tibetan Plateau, but their causes are still not very clear.

The geophysical results obtained so far are usually not consistent with each other, indicating that our understanding of the evolution of the Tibetan plateau is still incomplete. To date, most of the research projects have carried out geophysical observations in central and eastern Tibet, whereas there have been few such observations in western Tibet. In this study, we apply P-wave anisotropic tomography to the data recorded by the seismic stations deployed along the ANTILOPE-I (Array Network of Tibetan International Lithospheric Observation and Probe Experiment) profile in western Tibet and the southern Tarim basin (Fig. 1). Our results shed new light on the extending distances and properties of the Indian and Eurasian plates, as well as the deformation mode in the crust and upper mantle beneath western Tibet.

2. Data and method

2.1. Data selection

We used well-located local and teleseismic events recorded at 68 portable seismic stations of the ANTILOPE-I profile, which were deployed from October 2006 to November 2007 (Fig. 1). We manually picked up P- and S-wave arrival times (including Pg, Pn, P, Sg, Sn, and S phases) using the Crazyseismic software which is based on the waveform cross-correlation. By performing different frequency band-filtering, the picking accuracy is estimated to be 0.1–0.2 s for P-wave data and 0.2–0.3 s for S-wave data. Theoretical travel times are calculated using the iasp91 Earth model (Kennett and Engdahl, 1991) for the upper mantle and a modified CRUST1.0 model (Laske et al., 2013) for the crust (Fig. 2a). Hypocentral parameters of the teleseismic events were determined by the United States Geological Survey, whereas those of the local and regional events were determined by the China Earthquake Network Center (CENC). The selected teleseismic events have magnitudes greater than 5.5, and their epicentral distances are restricted between 30° and 90° from the center of the study area (Figs. 1b and 1c). For the local earthquakes, we selected only the events with magnitudes greater than 4.0, and we eliminated those poorly located events with a fixed focal depth of 33 km by the CENC. It was difficult to identify the precise arrivals of local earthquakes, hence we bandpass-filtered the original seismograms in different frequencies and adopted the average arrival time in the inversion. In addition, we only collected those arrival times with a clear onset, and all the phases used in this study are the first arrivals. In practice, the complex geometry of the Moho discontinuity and velocity variations in the lower crust beneath the study region often make it hard to distinguish the upper-mantle P-wave arrivals from the Pn-wave arrivals. Therefore, we took several processing steps to measure Pn and Sn arrival times (Hearn, 1996). The Pn and Sn data were collected based on the following criteria: (1) epicentral distances between 3°∼11°; (2) the focal depth is smaller than the Moho depth which is determined from the CRUST1.0 model; (3) the Pn wave travel-time residual is <4 s (and <5 s for Sn wave) after a straight line fit; (4) each event was recorded by at least 8 stations; and (5) each station recorded at least 8 local or regional events. The maximum epicentral distance is restricted to 11°, because the travel-time residuals for the initial velocity model form a straight line up to 11° in a residual-distance plot. The minimum epicentral distance is restricted to 3° rather than 1.5° because of the thick crust beneath Tibet.

The Vp/Vs ratio is calculated directly from the separate Vp and Vs models in an area with a good ray coverage for both P and S waves. Differences in the coverage of P- and S-wave rays can lead to different resolutions of Vp and Vs models, which may result in uncertainties in Vp/Vs ratio. Hence, we chose only those events which have both of clear P- and S-wave arrivals.